SAND2018-11908C

Predictive Modeling of Bolted Assemblies with Surface Irregularities

Matthew Fronk
Department of Mechanical Engineering
Georgia Institute of Technology
Atlanta, GA

Gabriela Guerra
Department of Mechanical & Aerospace Engineering
New Mexico State University
Las Cruces, NM

Matthew Southwick
Department of Mechanical Engineering
University of Pittsburgh
Pittsburgh, PA

Robert J. Kuether
Sandia National Laboratories
Albuquerque, NM

Adam Brink
Sandia National Laboratories
Albuquerque, NM

Paolo Tiso
ETH Zurich
Zurich, Switzerland

Dane Quinn
The University of Akron
Akron, OH

ABSTRACT

Bolted interfaces are a major source of uncertainty in the dynamic behavior of built-up assemblies. Contact pressure distribution from a bolt's preload governs the stiffness of the interface. These quantities are sensitive to the true curvature, or flatness, of the surface geometries and thus limit the predictive capability of models based on nominal drawing tolerances. Fabricated components inevitably deviate from their idealized geometry; nominally flat surfaces, for example, exhibit measurable variation about the desired level plane. This study aims to develop a predictive, high-fidelity finite element model of a bolted beam assembly to determine the modal characteristics of the preloaded assembly designed with nominally flat surfaces. The surface geometries of the beam interface are measured with an optical interferometer to reveal the amount of deviation from the nominally flat surface. These measurements are used to perturb the interface nodes in the finite element mesh to account for the true interface geometry. A nonlinear quasi-static preload analysis determines the contact area when the bolts are preloaded, and the model is linearized about this equilibrium state to estimate the modal characteristics of the assembly. The linearization assumes that nodes/faces in contact do not move relative to each other and are enforced through multi-point constraints. The structure's natural frequencies and mode shapes predicted by the model are validated by experimental measurements of the actual structure.

Keywords: Modal analysis; preload analysis; bolted joints; perturbed mesh; interface stiffness

1 INTRODUCTION

The dynamic behavior of monolithic structures can be accurately modeled using conventional and well-established computational and analytical tools such as finite element analysis. However, the presence of joints and mechanical interfaces adds an appreciable degree of uncertainty to the dynamic behavior of a mechanical system and presents significant modeling challenges. Since the use of joints in design is ubiquitous, it is imperative to develop accurate models to predict the structural dynamic response of assembled systems that include bolted interfaces.

Many studies have investigated the uncertainty associated with the vibration of jointed structures. Paez *et al.* characterized the variability of the natural frequencies of a cantilever clamped beam with a bolt and washer using combined finite element analysis and experimental data [1]. Uncertainties in the parameters of non-ideal (*i.e.,* flexible, non-rigid) boundary conditions have been investigated in [2, 3]. Fuzzy set theory has been applied to quantify the uncertainty of joint stiffness and damping [4, 5]. A review of the uncertainties in the prediction of dynamic response of jointed structures can be found in [6]. The literature, however, does not quantify the effect of surface waviness on the dynamic properties of a jointed structure or its associated uncertainty on experimental measurements. Bickford discusses that tightening joints composed of non-parallel or warped members hinders the accuracy of torque-preload relationships [7], but does not address its effect on the dynamic response of the assembly.

A common technique to improve the accuracy of computational models is model updating, wherein experimental test data is used to adjust—or update—model parameters. An overview of the model updating procedure applied to structural dynamics problems is found in [8]. When calibrating linearized models of jointed structures, prior studies have optimized the values of springs, masses, and dampers at the model's interface to match modal characteristics measured from actual hardware [9-12]. Additional techniques include varying geometric parameters [13] as well as the material properties of a "doubly connective layer" [14]. Some of the authors recently published a study that proposed a model updating routine in which the contact definitions of elements at the nonlinear interface were varied (*e.g.* stuck, slipping or no contact) as a function of their normal contact pressure magnitude [15]. In comparison to modal test data, close agreement across six elastic modes was obtained for an optimal value of the model's "cut-off pressure", which was a single, scalar value used to assign the appropriate multi-point constraints. The current work expands on this study by performing model updating of individual beams to reduce the uncertainty of material properties, and evaluates the predictive capability of an FE model of the preloaded assembly when surface waviness at the interface is included.

A variety of techniques have been documented for modeling joint behavior in computational studies. In [16], two different multi-point constraint (MPC) configurations are compared in the calculation of the vibration modes of an automobile engine. The first confines member stiffness to be around each bolt hole and the second distributes member stiffness across the entire joint interface. The second configuration produces better agreement with the first two flexible modes of the actual engine. Four different approaches for modelling bolts in jointed structures were compared in [17]: a solid model of the bolt with solid elements, rigid spiders coupling the nodes around the bolt hole, a web of beam elements, and a constant preload force applied to the washer

surfaces. While the most computationally expensive, the approach incorporating solid elements for the bolt produced the best agreement with static and dynamic test measurements. Other models characterizing the nonlinear effects of joints have been developed over recent years [18-21], but these studies are beyond the scope of this work since this work focuses on linear vibration responses at low excitation levels.

This paper presents the development of a high-fidelity finite element (FE) model of a jointed structure, with the aim of determining the effect of surface waviness at the interface on the assembled system's natural frequencies. A benchmark structure consisting of two steel beams with nominally flat interfaces is studied, and a roving hammer impact test provides its linear natural frequencies and mode shapes for validation. Individual beams and fasteners are calibrated in isolation to obtain their material properties. In the FE model of the bolted assembly, nodes along the contact surfaces are perturbed based on measurements of surface heights on the actual beams. A brief outline of the paper is as follows: Section 2 describes the benchmark structure studied in this work. Section 3 outlines the model updating procedures carried-out on individual system components to minimize uncertainties due to material properties and interface geometry. Section 4 presents the results of the experimental modal analysis on the bolted assembly as well as the computational results of the model with the updated parameters and surface geometry from Section 3. The natural frequency predictions of the updated computational model are then compared to the measurements in the actual bolted assembly. Comparisons with the accuracy of other computational modelling approaches for the jointed structure are made.

2 SYSTEM DESCRIPTION

Figure 1 depicts the bolted assembly considered in this study. The beams are manufactured from 4340 alloy steel and each are prescribed to have the same dimensions provided in Appendix A. The raised pads at the beams' ends create well-defined regions of contact for the bolted interface. The assembled bolted structure uses two 5/16"-24 UNF-2B bolts and its associated nut and washer to fasten the individual beams at each end. Additionally, the beams were assigned serial numbers B9A and B9B to facilitate the model updating process. A flatness tolerance of 0.001" was imposed on the manufacturing drawing to minimize the deviations from a nominally flat interface.

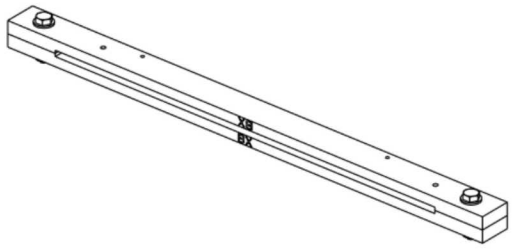

Figure 1. Isometric view of bolted C-beam assembly

3 SINGLE BEAM STRUCTURE

The details of this experiment and model calibration of the individual beams are given in Sections 3.1 and 3.2.

3.1 EXPERIMENTAL MODAL ANALYSIS

Roving impact hammer testing was performed on each of the individual beams to fit the natural frequencies and mode shapes. Figure 2 shows the test setup and reference coordinate grid for a single beam structure without any bolt hardware. The single beam was suspended by bungee cords to approximate free-free boundary conditions. Impacts from a roving hammer were carried out at a total of thirty-three input points in both the y and z directions. To maintain linearity of the response, the impacts were performed at low force levels around 11 lbf for all test points.

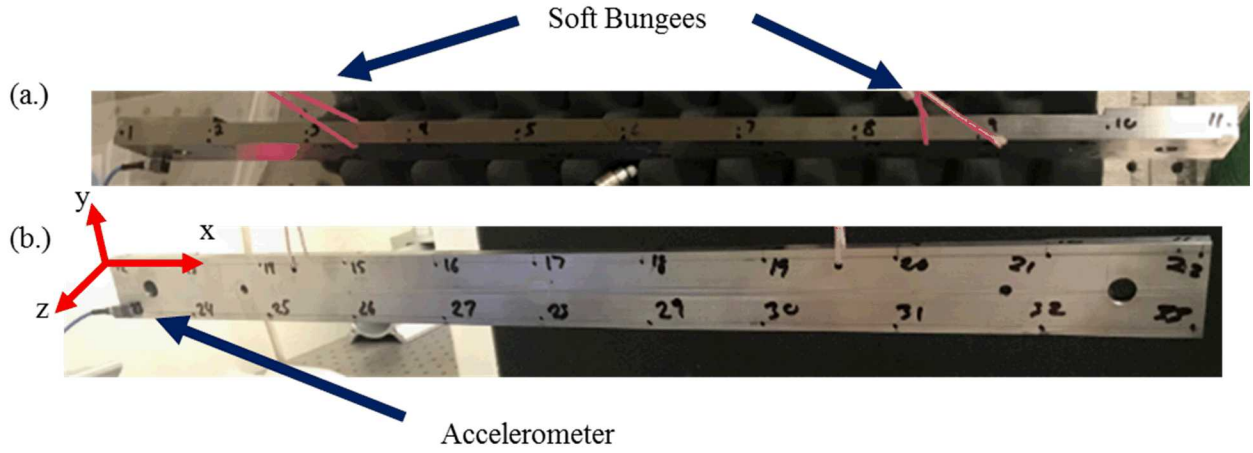

Figure 2: Roving hammer impact test set-up for the single beam structure. (a.) Top view, (b.) Front view

The natural frequencies and mode shapes for the first five elastic modes are presented in Table 1 for beam subcomponents B9A and B9B. The experimental modes were extracted using the LMS "PolyMAX" tool, a polyreference least squares frequency domain modal parameter estimation method [22, 23]. Note the slight variation between the frequencies of B9A and B9B, which are likely due to small differences in their material properties. These results are compared to predictions from a high-fidelity FE model of the individual beams with nominal geometry and material properties (Young's modulus of 29,000 ksi, Poisson's ratio of 0.283, and density of 7.12E-04 slug/in^3 [24]). Moderate agreement is obtained with these experimental measurements: the 3rd y-bending mode possessed the highest amount of error in its natural frequency of 1.2% whereas the 1st torsional mode possessed the lowest diagonal modal assurance criterion (MAC) value of 49.9%.

Table 1. Natural frequencies [Hz] for the individual beams: experimental measurements compared to FE model with no updating

Mode	Natural Frequency [Hz]		
	Beam 9A	Beam 9B	FE (Nominal Beams)
1st y-bending	187.5	187.1	189.3
2nd y-bending	526.3	525.1	523.3
3rd y-bending	610.8	610.3	603.8
1st z-bending	1042.7	1042.8	1037.9
1st Torsion	1545.5	1541.8	1530.7

3.2 MODEL UPDATING

To further reduce the error between the model's predicted natural frequencies and those measured in the individual beams, model updating of the material properties of all subcomponents used in the final assembly was performed. As a result, sources of uncertainty outside of the mechanical interfaces were eliminated.

3.2.1 DENSITY

The first material property updated in the FE model was mass density. Each individual beam and fastener were weighed to obtain the mass, and the density of each subcomponent was calculated by dividing each mass by its associated volume estimated from the FE model. It was assumed that the small deviations from nominal dimensions of the beams have a negligible effect on their overall volume and thus were not included in these calculations. The updated densities were used in the material property definitions of the linear elastic constitutive model. Furthermore, each bolt, nut, and washer were serialized to maintain consistency in the structure's configuration during assembly/reassembly and in the FE model. Table 2 lists the mass measurements and density calculations for all the components.

Table 2. Sub-component mass measurements and density calculations.

	Beam		Bolt		Nut		Washer			
	B9A	B9B	Right	Left	Right	Left	Top Right	Bottom Right	Top Left	Bottom Left
Mass [Slug]	7.3E-03	7.3E-03	1.0E-04	1.0E-04	2.87E-05	2.8E-05	1.1E-05	1.2E-05	1.1E-05	1.2E-05
Density [Slug/in^3]	7.3E-04	7.4E-04	6.7E-04	6.7E-04	9.1E-04	9.0E-04	6.3E-04	6.4E-04	6.3E-04	6.4E-04

3.2.2 YOUNG'S MODULUS

The elastic modulus of each beam was optimized in the FE model using the natural frequencies measurements from the roving hammer modal tests. The FE model included a point mass to account for the mass loading from the single accelerometer used during testing. The Young's modulus values that minimize the least squares error with the measured natural frequencies are 30,850 and 30,470 ksi for B9A and B9B, respectively. These values are approximately 6% and 5% larger than the nominal value of 4340 steel which is 29,000 ksi. Table 3 compares the experimental and material property-updated FE natural frequencies for B9A and B9B.

Table 3. Natural frequencies from the experiment and FE model with updated density and Young's modulus values. Percent errors of the FE model predictions are listed in parenthesis.

Mode	B9A Natural Frequency [Hz]		B9B Natural Frequency [Hz]	
	Experimental	Young's Modulus Updated FE	Experimental	Young's Modulus Updated FE
1st y-bending	187.5	187.7 (+0.1%)	187.1	187.3 (+0.1%)
2nd y-bending	526.3	527.4 (+0.2%)	525.1	526.4 (+0.2%)
3rd y-bending	610.8	608.1 (-0.4%)	610.2	606.9 (-0.5%)
1st z-bending	1042.7	1046.5 (+0.4%)	1042.9	1044.5 (+0.2%)
1st torsion	1545.6	1541.8 (-0.2%)	1541.8	1538.8 (-0.2%)

3.2.3 SURFACE GEOMETRY

While tight tolerances were imposed on the fabricated beams, their geometry will inevitably deviate from the nominally flat design due to a number of factors during machining including vibration and deformation of the machine tools, insufficient clamping, and workpiece material inhomogeneities [25]. These deviations from the ideal flat surface were incorporated into the FE models of the beams to investigate their influence on the contact pressure distribution in the bolted assembly. Optical interferometer measurements generated high-resolution surface profile data for each of the four contact surfaces (two raised pads for each beam). Figure 3 presents images of the surface measurements in which hotter colors correspond to deviations above the level plane while cooler colors correspond to deviations below the level plane.

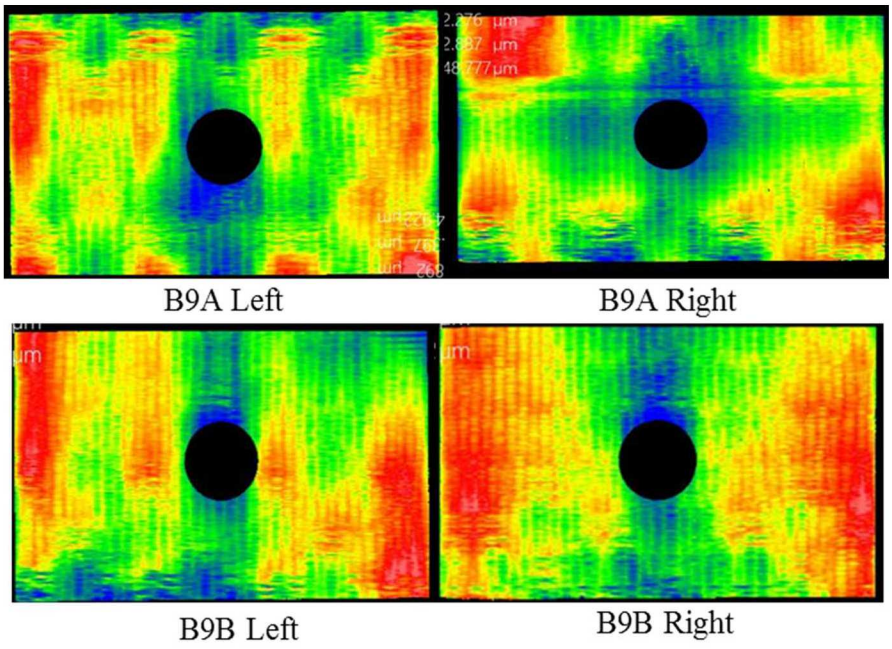

Figure 3. Optical interferometer measurements of the beam surfaces. Hotter colors correspond to surface heights that are above the level plane while cooler colors correspond to surface heights below the level plane.

Figure 4 plots a line scan about the center of the raised pad to provide insight into the data of the surface deviation. For each node on the contact surfaces, the nearest coordinate, in the roughly 8,000 by 5,000 grid of measurements, was located and its corresponding surface height extracted. This array of deviated surface heights was used to update the nodal coordinates in the FE mesh. Each node was matched with a data point in the optical interferometer measurements with the closest coordinates and perturbed to have the corresponding amount of surface height deviation.

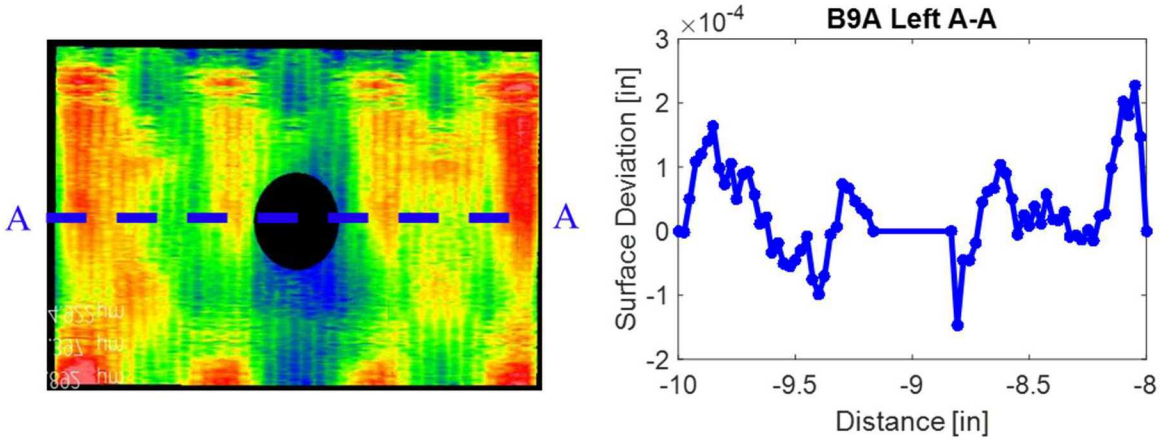

Figure 4. Line scan of the surface displaying the magnitude of the deviation about the level plane from optical interferometer measurements

4 BOLTED BEAM ASSEMBLY

After minimizing the error between the computational model and experimental measurements of the individual beams, the bolted assembly was investigated to understand the influence of the interface geometry on the modes of the bolted assembly. Details of the experimental and computational analysis of the bolted assembly are provided here, concluding with a discussion of the predictive capability of different FE modelling approaches.

4.1 EXPERIMENTAL MODAL ANALYSIS

Modal testing was performed on the bolted assembly to extract linear natural frequencies and mode shapes at low excitation levels. Figure 5 depicts the experimental test setup. The assembly was supported with bungee cords to approximate free-free boundary conditions. Impact forces were applied in the y and z directions at sixty-six distributed points to accurately resolve the mode shapes along the length of the beam. Two triaxial accelerometers measured the accelerations for each impact point. Bolts were tightened to 110 in-lbf using a torque wrench and Table 4 provides a summary of the first eight elastic modes of the bolted beam assembly.

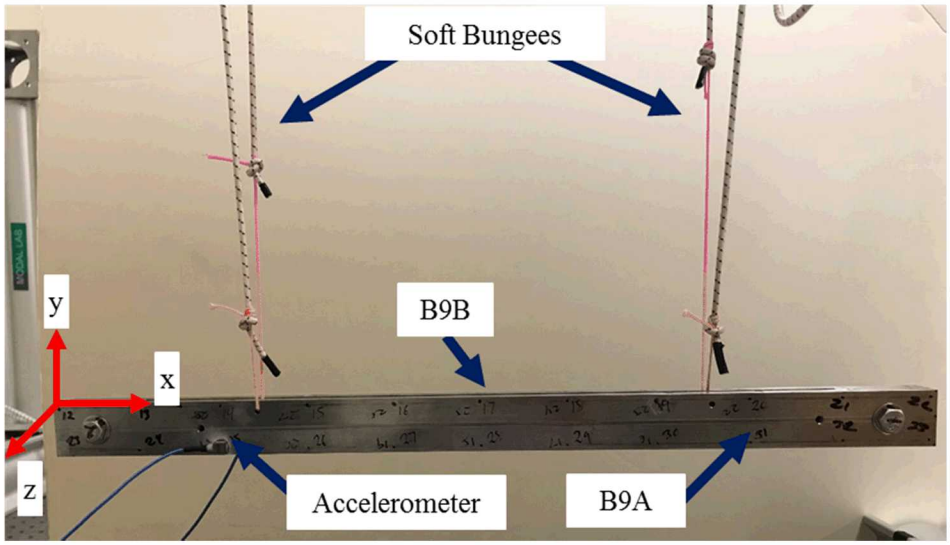

Figure 5. Roving hammer impact test set-up for the bolted beam assembly

A linearity study was conducted to ensure the natural frequencies were extracted from hammer input levels known to excite linear vibration responses. The purpose of this study is to identify input forces that produce linear responses with little to no change in the system's measured frequency response function (FRF). The structure was impacted at a range of forces between 3 to 40 lbf and the measured FRF's from the different impact levels were visually compared. Figure 6 depicts the two forms of nonlinear responses observed in specific modes. The first type of nonlinear response is characterized by an opening/closing of the interface at higher input levels, which produced a shift in peak frequency and increase in FRF magnitude resulting from the apparent decrease in stiffness and damping during vibration. The 1st and 2nd out-of-phase y-bending modes exhibited this behavior. The second type of nonlinear response resulted from shear loads at the interface resulting in significant energy dissipation due to friction. Figure 6b shows

how the 1st out-of-phase z-bending mode exhibits this behavior. Higher input levels produced a reduction in FRF magnitudes and an apparent decrease in peak frequency. The remaining results for the linearity study are provided in Appendix B.

In contrast to the behavior observed with the 1st out-of-phase z-bending mode, the 1st in-phase z-bending mode was inherently linear as evidenced by the FRF consistency across all input force levels. As apparent in its mode shape deformations, the 1st in-phase z-bending mode does not induce significant stresses at the interface when compared to the other modes. Between 3.5 and 14.2 lbf, the natural frequencies observed from the peak points of the FRF remain essentially unchanged with less than 1 Hz shifts. Only the damping levels seemed to be significantly affected by the input level. For all the results from the linearity study, it appeared that it was difficult to apply a low enough input force the excite the structure in such a way that linearity of the response can be confirmed via visual inspection of the FRF. The experimental modes used for validation purpose were fit from the FRFs obtained from the lowest possible input forces in hopes that these best approximate the linear response. This seemed reasonable since the natural frequencies were of most interest to understand the effect of surface geometry on the joint stiffness.

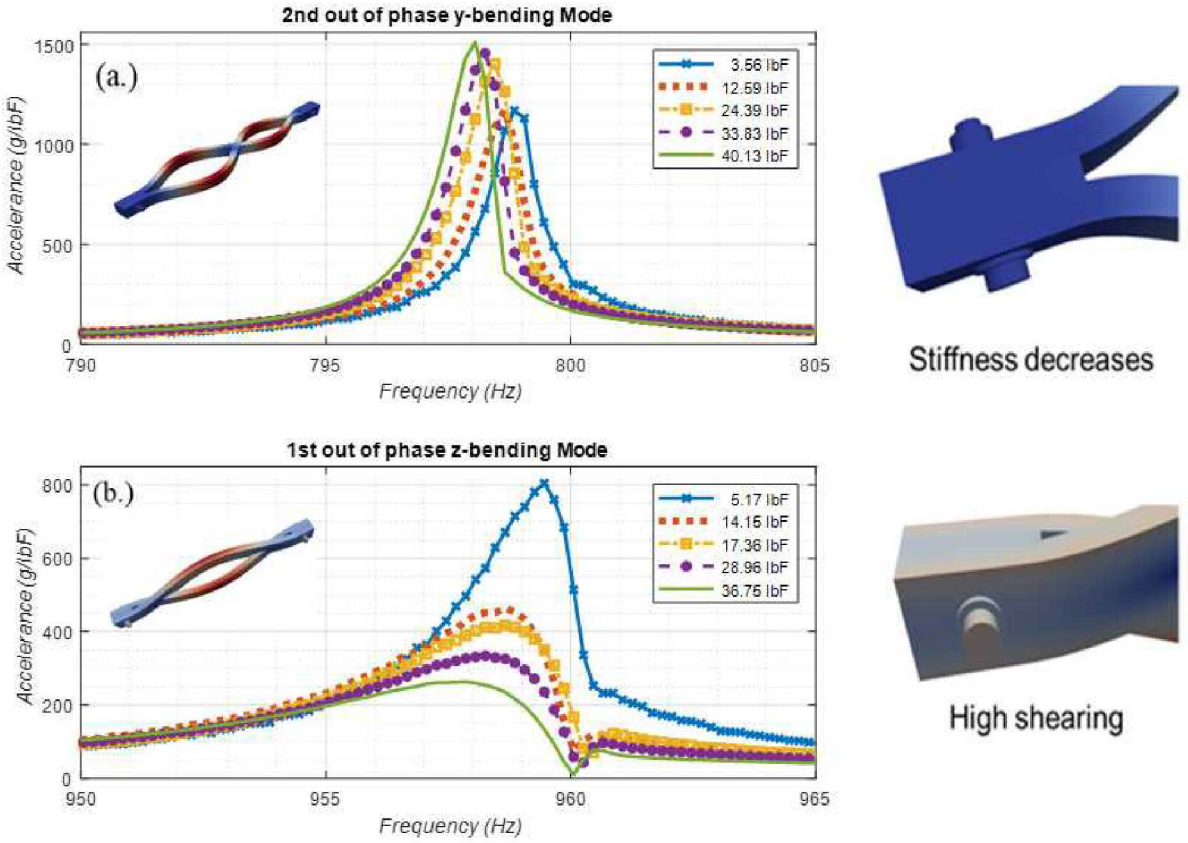

Figure 6. Two classes of nonlinear behavior observed in the measured FRF's of the bolted assembly: (a.) stiffness decrease due to opening of the interface (b.) high dissipation due to shearing forces at the interface

4.2 COMPUTATIONAL PRELOAD ANALYSIS

The FE model was preloaded by applying an axial force along the bolt shank, then gluing the nut to the shank, thus locking in the preload. The conversion from torque to axial preload was determined using the Motosh equation [26]. This method produced the 2400 lbf preload used in the model. It should be noted that there is considerable uncertainty in the joint preload with a torque wrench. The preload force in an unlubricated bolt tightened with a torque wrench has been shown to be possess a 35% uncertainty its predicted value [27].

Figure 7 presents the results of the preload analysis for the nominally flat surfaces. Note that the contact pressure is largest around the bolt hole and decreases further away from it, forming concentric rings of pressure. Such a contact area is characteristic of receding contact in which the area remains independent of the load while the pressures scale linearly with the load [28].

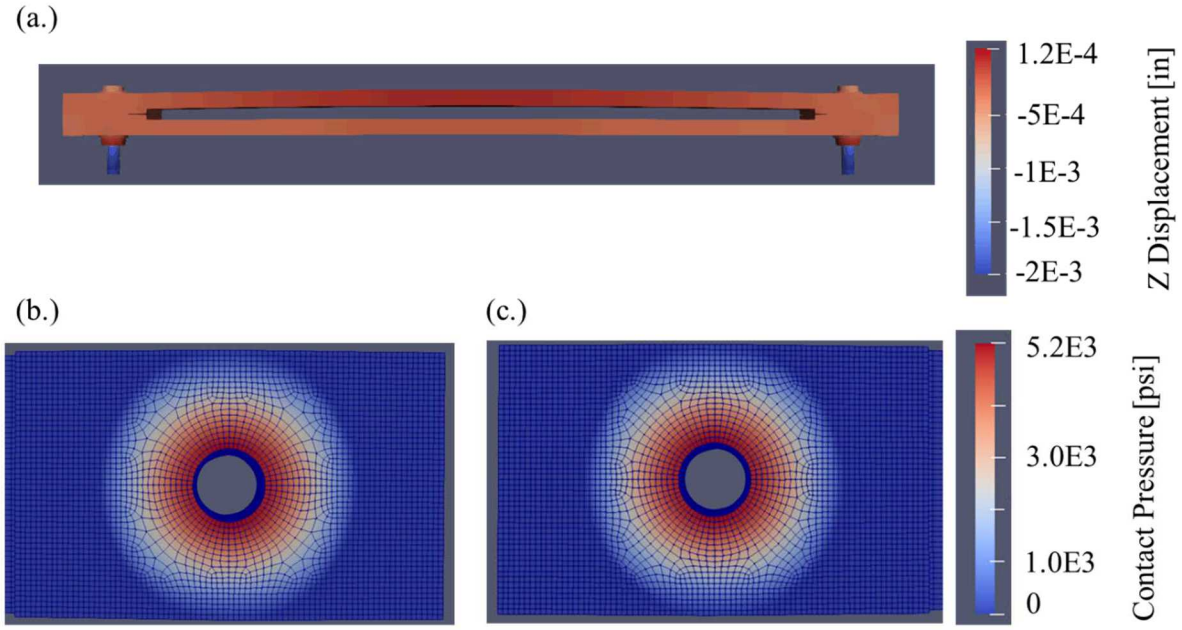

Figure 7. Results of the static preload FE analysis for the flat beam assembly. (a.) Z displacements in the structure (b.) Left side contact pressure at the beam/beam interface (b.) Right side contact pressure at the beam/beam interface

Figures 8 and 9 present the results of the preload analysis for the surfaces with irregularities. The resulting contact area is markedly different than that of the nominally flat case. Zones of high contact pressure loosely correspond to regions near the bolt hole with large surface deviations.

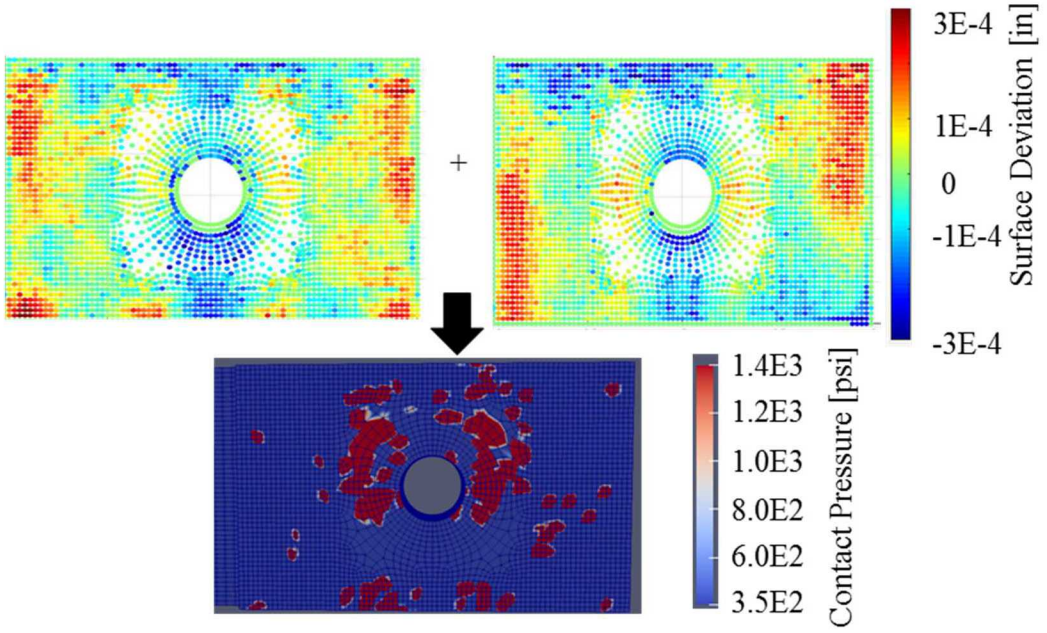

Figure 8. Computationally-determined interface contact pressure for the left side of the bolted beam assembly

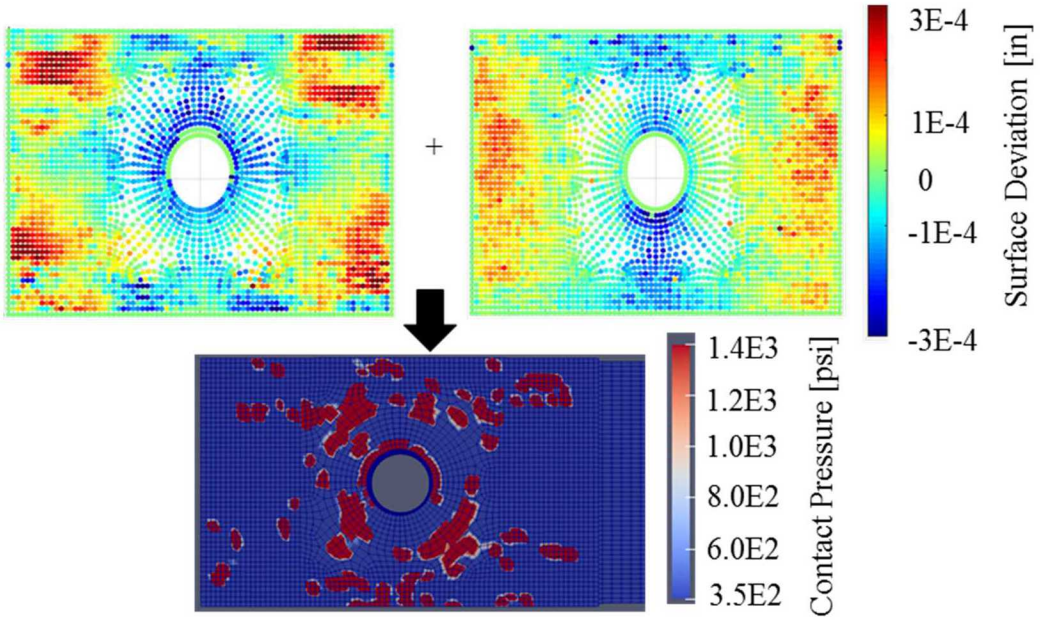

Figure 9. Computationally-determined interface contact pressure for the right side of the bolted beam assembly

The results from the preload analysis on the non-flat geometry are compared to digitized pressure film measurements in the actual beam assembly. These films were inserted in the interface and output contact pressures between 350 and 1400 psi after applying the torque to the bolts. Figure 10 displays the results. While they are not in complete agreement, note that the model for the left

side captures the two "strips" of high pressure to the left and right sides of the bolt hole. This agreement looks qualitatively better than the nominally flat results, which suggest the pressures are distributed in concentric rings around the bolt hole.

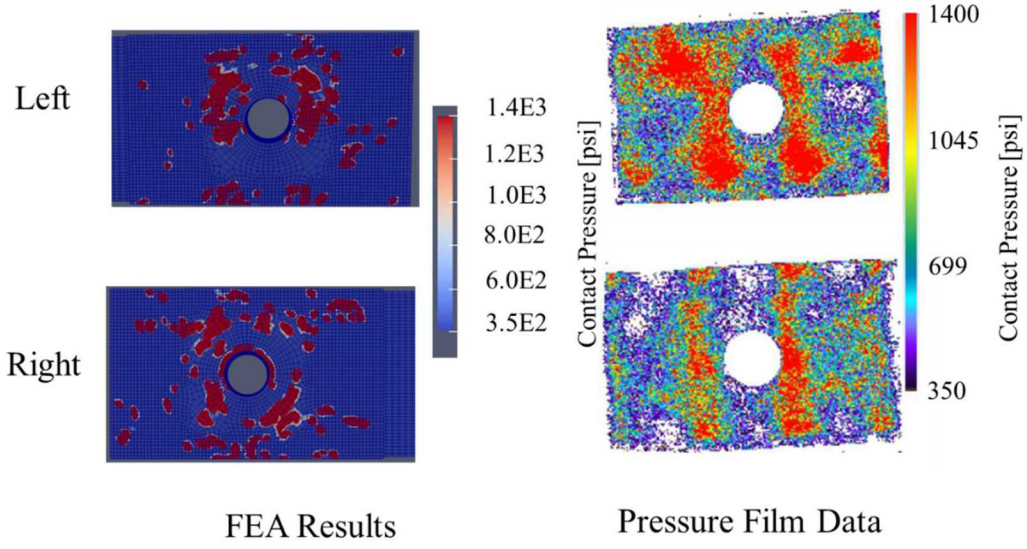

Figure 10. Computationally-determined contact pressures compared to digitized pressure film measurements in the actual beam assembly

4.3 MODAL ANALYSIS VALIDATION

The results from the preload analysis are transferred into the Sierra Structural Dynamics FE code [29] to perform modal analysis and calculate the linearized natural frequencies and mode shapes. It was assumed that the bolt preload was high enough such that regions in contact remained in contact during vibration. Thus, rigidly tied multi-point constraints were applied to all nodes surrounding elements in contact. Additionally, both structural damping and dissipation caused by relative motion at the interface were neglected. Free-free boundary conditions were prescribed to the model to match the approximate boundary conditions from test.

Table 4 compares the natural frequency predictions of each of the computational models relative to the experimental measurements. Each computational model incorporates higher complexity in its description of contact and surface geometry. The percent error of each computational prediction of natural frequency relative to the experimental value is listed in parenthesis. The simplest modeling approach—flat surface, fully stuck—defined all nodes on the perfectly flat raised pads to be rigidly tied together, enforced by multi-point constraints. Such configuration overpredicts the natural frequencies as it has much larger stiffness than the actual structure. The second modelling approach—flat surface, preloaded—uses the static preload results on the flat beams to determine which nodes are tied together using the method described in Section 4.2. With this approach, a constant ring of stuck elements was formed around the bolt hole, which offers the most accurate natural frequency predictions for the in-phase y-bending modes. The most complicated modelling approach—perturbed surfaced, preloaded—updates the surface geometry based on the

surface deviation data and then runs the static preload analysis to determine the distribution of struck and free nodes at the interface. This method offers an order of magnitude reduction in the error of its natural frequency predictions relative to the flat surface case for the out-of-phase y and z-bending modes.

Table 4. Comparison of natural frequency predictions from different FE models to experimental measurements. Percent error between natural frequencies from the FE models and experimental measurements are displayed in parenthesis.

	Flat surface, fully stuck **[Hz]**	***Flat surface, preloaded*** **[Hz]**	***Perturbed surface, preloaded*** **[Hz]**	***Experiment*** **[Hz]**
Mode Shape			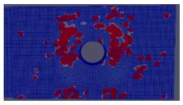	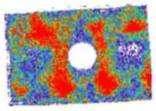
	297.0 (+2.2%)	283.0 (-2.6%)	289.2 (-0.4%)	290.4
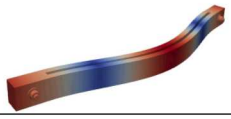	359.2 (+1.5%)	354.5 (+0.2%)	355.5 (+0.5%)	353.8
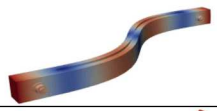	513.9 (+1.1%)	513.3 (+1.0%)	513.5 (+1.0%)	508.4
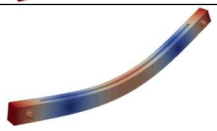	597.0 (-0.3%)	597.0 (-0.3%)	597.1 (-0.3%)	598.6
	814.6 (+2.1%)	773.0 (-3.2%)	791.6 (-0.8%)	797.6
	982.9 (+2.8%)	925.9 (-3.2%)	948.7 (-0.7%)	955.6
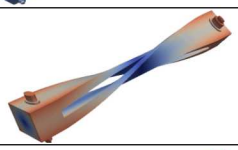	1183.7 (-0.2%)	1176.0 (-0.8%)	1178.9 (-0.6%)	1185.6
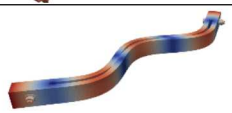	1359.4 (+1.1%)	1353.0 (+0.6%)	1353.7 (+0.7%)	1344.4

For all the modes in which the perturbed surface model has a higher level of accuracy compared to the flat surface model, the stiffness of the structure increases to raise the natural frequency. Such trend may be due to the points far away from the bolt hole that have high surface deviation and therefore come into contact during the static preload. A receding contact model cannot capture these points and thus may under-predict the joint's stiffness. If out-of-phase bending modes are desired to be predicted by a model, the perturbed surface approach may be the most attractive candidate in applications where a high-degree of accuracy is demanded. However, this modeling approach requires special equipment to measure surface deviations which may not be readily available or such measurements may not be easily carried-out for large and complex engineering structures.

5 CONCLUSIONS

A high-fidelity FE model of a bolted beam assembly was developed, calibrating the material properties of individual beams and fasteners with experimental measurements and perturbing nodal coordinates at the interface with surface height measurements from an optical interferometer. A preload analysis determines the distribution of contact pressure in the interface and consequently which nodes/faces are tied together. Significant improvements in the model's predictions of natural frequency for the actual beam system are observed in out-of-phase bending modes, likely due to perturbed surface heights coming into contact far away from the bolt hole, a phenomenon unable to be captured by a receding contact description for nominally flat surfaces. This high-fidelity modelling method could be implemented in applications where enhanced predictive capability is important.

While finer meshes capture more detail in the surface topographies, it is advised in future studies to employ an averaging method to the mesh perturbation such that a small neighborhood of points in the data file are averaged for each nodal coordinate. Doing so would account for outliers in the measured data from specks of dust or large angles in the surface (for low magnification lenses) or points located on edges. Additionally, it is suggested to consider surface geometries with a prescribed curvature instead of those that are nominally flat to investigate the robustness of this method.

ACKNOWLEDGMENTS

This research was conducted at the 2018 Nonlinear Mechanics and Dynamics (NOMAD) Research Institute supported by Sandia National Laboratories. Sandia National Laboratories is a multi-mission laboratory managed and operated by National Technology and Engineering Solutions of Sandia, LLC., a wholly owned subsidiary of Honeywell International, Inc., for the U.S. Department of Energy's National Nuclear Security Administration under contract DE-NA-0003525. The authors would also like to thank Bill Flynn from Siemens Industry Software NV for supplying the data acquisition and testing systems used to collect the experimental measurements presented throughout this work.

APPENDIX A

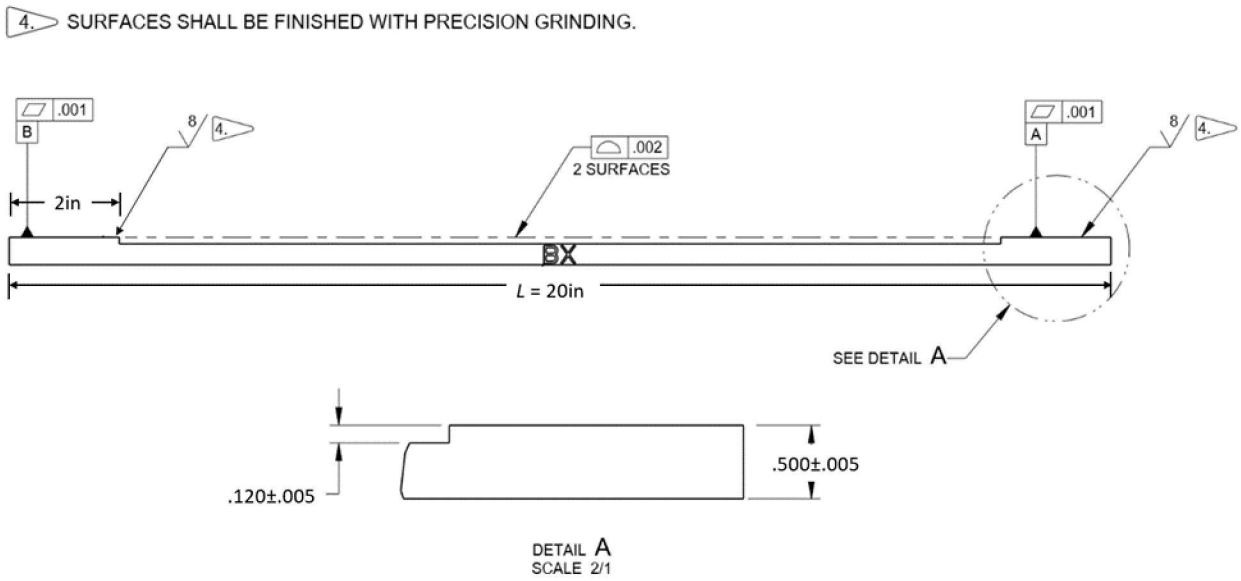

Figure 11. Dimensions of the individual beams

APPENDIX B

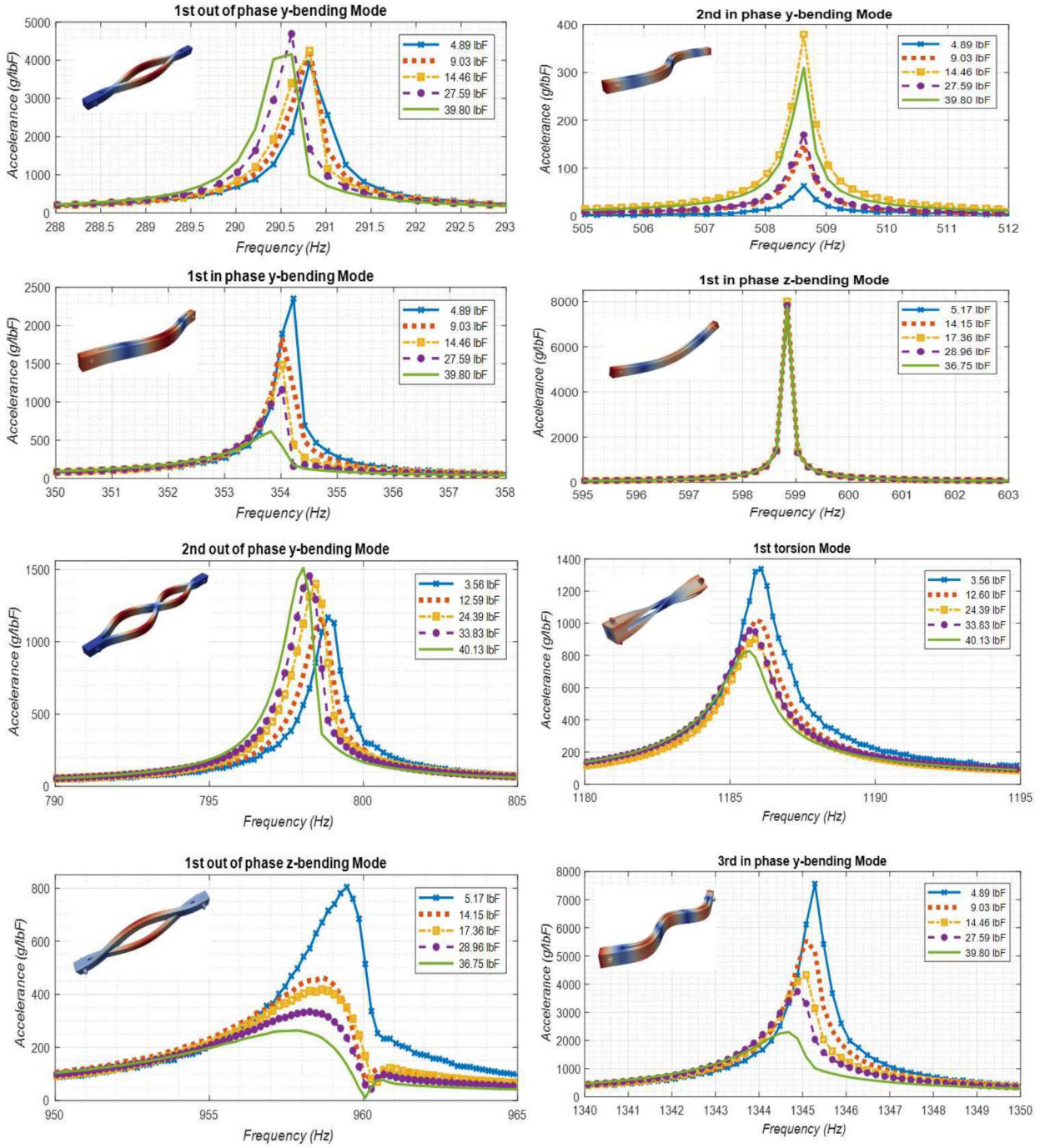

Figure 12. Linearity study of the bolted beam assembly

References

[1] **Paez, T. L., Branstetter, L. J.,** and **Gregory, D. L.**, *Modal Randomness Induced by Boundary Conditions,* SAE Technical Paper No. 851930, 1985.

[2] **Fengquan, W.,** and **Shiyu, C**., *A Method to Determine the Boundary Conditions of the Finite Element Model of a Slender Beam Using Measured Modal Parameters*, Journal of Vibration and Acoustics, 118 (3), pp. 474-478, 1996.

[3] **Lee, U.,** and **Kim, J**., *Determination of Nonideal Beam Boundary Conditions: A Spectral Element Approach*, AIAA Journal, 38 (2), pp. 309-316, 2000.

[4] **Hanss, M**. *Simulation and Analysis of Structural Joint Models with Uncertainties*, Proc. of the International Conference on Structural Dynamics Modeling-Test, Analysis, Correlation and Validation, Madeira Island, Portugal, 2002.

[5] **Hanss, M., Oexl, S.,** and **Gaul, L**., *Identification of a Bolted-Joint Model with Fuzzy Parameters Loaded Normal to the Contact Interface*, Mechanics Research Communications, 29 (2-3), pp. 177-187, 2002.

[6] **Ibrahim, R. A.,** and **Pettit, C. L**., *Uncertainties and Dynamic Problems of Bolted Joints and Other Fasteners*, Journal of Sound and Vibration, 279 (3), pp. 857-936, 2005.

[7] **Bickford, J**., *An Introduction to the Design and Behavior of Bolted Joints, Revised and Expanded*, Routledge, 2018.

[8] **Mottershead, J. E.,** and **Friswell, M**., *Model Updating in Structural Dynamics: A Survey*, Journal of Sound and Vibration, 167 (2), pp. 347-375, 1993.

[9] **Mottershead, J. E.,** and **Weixun, S**., *Correction of Joint Stiffnesses and Constraints for Finite Element Models in Structural Dynamics*, Journal of Applied Mechanics, 60 (1), pp. 117-122, 1993.

[10] **Kim, T., Wu, S.,** and **Eman, K**., *Identification of Joint Parameters for a Taper Joint*, Journal of Engineering for Industry, 111 (3), pp. 282-287, 1989.

[11] **Kim, T., Ehmann, K.,** and **Wu, S**., *Identification of Joint Structural Parameters between Substructures*, Journal of Engineering for Industry, 113 (4), pp. 419-424, 1991.

[12] **Nobari, A. S., Robb, D.,** and **Ewins, D**., *Model Updating and Joint Identification Methods-Applications, Restrictions and Overlap*, International Journal of Analytical and Experimental Modal Analysis, 8, pp. 93-105, 1993.

[13] **Mottershead, J., Friswell, M., Ng, G.,** and **Brandon, J**., *Geometric Parameters for Finite Element Model Updating of Joints and Constraints*, Mechanical Systems and Signal Processing, 10 (2), pp. 171-182, 1996.

[14] **Adel, F., Shokrollahi, S., Jamal-Omidi, M.,** and **Ahmadian, H**., *A Model Updating Method for Hybrid Composite/Aluminum Bolted Joints Using Modal Test Data*, Journal of Sound and Vibration, 396, pp. 172-185, 2017.

[15] **Fronk, M., Eschen, K., Starkey, K., Kuether, R. J., Brink, A., Walsh, T., Aquino, W**., and **Brake, M**., *Inverse Methods for Characterization of Contact Areas in Mechanical Systems*, Nonlinear Dynamics, Volume 1, Springer, 2019.

[16] **Langer, P., Sepahvand, K., Guist, C.,** and **Marburg, S**., *Finite Element Modeling for Structural Dynamic Analysis of Bolted Joints under Uncertainty*, Procedia Engineering, 199, pp. 954-959, 2017.

[17] **Kim, J., Yoon, J.-C.,** and **Kang, B.-S**., *Finite Element Analysis and Modeling of Structure with Bolted Joints*, Applied Mathematical Modelling, 31 (5), pp. 895-911, 2007.
[18] **Allen, M. S., Lacayo, R. M.,** and **Brake, M. R**., *Quasi-Static Modal Analysis Based on Implicit Condensation for Structures with Nonlinear Joints*, SAND2016-5065C, Sandia National Laboratories, Albuquerque, NM, 2016.
[19] **Flicek, R., Ramesh, R.,** and **Hills, D**., *A Complete Frictional Contact: The Transition from Normal Load to Sliding*, International Journal of Engineering Science, 92, pp. 18-27, 2015.
[20] **Segalman, D. J**., *A Four-Parameter Iwan Model for Lap-Type Joints*, Journal of Applied Mechanics, 72 (5), pp. 752-760, 2005.
[21] **Sellgren, U.,** and **Olofsson, U**., *Application of a Constitutive Model for Micro-Slip in Finite Element Analysis*, Computer Methods in Applied Mechanics and Engineering, 170 (1-2), pp. 65-77, 1999.
[22] **Peeters, B., Auweraer, H., Guillaume, P.,** and **Leuridan, J.**, *The PolyMAX Frequency-Domain Method: A New Standard for Modal Parameter Estimation?*, Shock and Vibration, Vol. 11, 3-4, pp. 395-409, 2004.
[23] *The LMS Test.Lab Modal Analysis Manual*, Rev12A, LMS International, pp. 30-31, 2012.
[24] **Bradley, R.**, *On the FEA via SNL Tools*, SAND2018-6567 O, Sandia National Laboratories, Albuquerque, NM, June 2018.
[25] **Benardos, P. G.,** and **Vosniakos, G. C.**, *Predicting Surface Roughness in Machining: A Review*, International Journal of Machine Tools and Manufacture, 43 (8), pp. 833-844, 2003.
[26] **Motosh, N.**, *Development of Design Charts for Bolts Preloaded up to the Plastic Range*, Journal of Engineering for Industry, 98 (3), pp. 849-851, 1976.
[27] **Brown, K., Morrow, C., Durbin, S.,** and **Baca, A**., *Guideline for Bolted Joint Design and Analysis: Version 1.0*, SAND2008-0371, Sandia National Laboratories, Albuquerque, New Mexico, 2008.
[28] **Dundurs, J.**, *Properties of Elastic Bodies in Contact*, The Mechanics of the Contact between Deformable Bodies, pp. 54-66, 1975.
[29] **Sierra Structural Dynamics Development Team**, *Sierra Structural Dynamics-User's Notes*, SAND2017-3553, Sandia National Laboratories, Albuquerque, NM, 2017.